

- GC(C/T)TGIC(T/G)ATCCACCA-3'] were synthesized and used for PCR amplification of *Cyanidium* total DNA. The reaction was performed with TAKARA Taq DNA polymerase (Takara Shuzo, Kyoto, Japan) for 30 cycles at 95°C for 1.5 min, 40°C for 2 min, and 72°C for 3 min. The amplified fragment was cloned with a pCR-Script SK cloning kit (Stratagene).
10. K. Tanaka, T. Shiina, H. Takahashi, *Science* **242**, 1040 (1988).
 11. N. Ohta, N. Sato, S. Kawano, T. Kuroiwa, *Curr. Genet.* **25**, 357 (1994).
 12. M. Lonetto, M. Gribskov, C. A. Gross, *J. Bacteriol.* **174**, 3843 (1992).
 13. K. Keegstra and L. J. Olsen, *Annu. Rev. Plant Physiol. Plant Mol. Biol.* **40**, 471 (1989); M. Reith, *ibid.* **46**, 549 (1995).
 14. To produce SigA in *E. coli* we inserted a 1733-bp Nde I-Bam HI fragment containing the *sigA* open reading frame into the linker site of the expression plasmid pET15b (Novagen) (15). The resultant plasmid, pETCA, was introduced into the host BL21(DE3) strain and the bacterial cells were incubated at 37°C in 300 ml of Luria broth (LB) medium until the optical density of the culture at 660 nm reached 0.5. Isopropyl- β -D-thiogalactopyranoside was then added to a final concentration of 0.5 mM, and after incubation for an additional 2 hours cells were collected by centrifugation. The recombinant protein was recovered as inclusion bodies, solubilized in TGED buffer [10 mM Tris-HCl (pH 8.0), 5% (w/v) glycerol, 0.1 mM EDTA, and 0.1 mM dithiothreitol] containing 6 M guanidine hydrochloride, and renatured by dialyzing against TGED buffer. The SigA protein was further purified in a fast protein liquid chromatography (FPLC) system (Pharmacia) on a POROS HQ column (4.6 mm \times 100 mm; PerSeptive Biosystems, Cambridge, MA). Elution was performed with a linear gradient of 0 to 1.0 M NaCl in the same buffer, and the peak fraction was precipitated with ammonium sulfate, dialyzed against storage buffer [TGED containing 0.5 M NaCl and 50% (w/v) glycerol], and stored at -30°C. The calculated molecular weight of the protein is 46,794 (440 amino acids).
 15. M. Studier, A. H. Rosenberg, J. J. Dunn, J. W. Dubendorff, *Methods Enzymol.* **185**, 60 (1990).
 16. K. Igarashi and A. Ishihama, *Cell* **65**, 1015 (1991).
 17. T. Nomura, N. Fujita, A. Ishihama, *Nucleic Acids Res.* **14**, 6857 (1986).
 18. H. Harlow and D. Lane, *Antibodies: A Laboratory Manual* (Cold Spring Harbor Laboratory, Cold Spring Harbor, NY, 1988).
 19. K. Tanaka and H. Takahashi, *Biochim. Biophys. Acta* **1089**, 113 (1991).
 20. K. A. Johnson and J. L. Rosenbaum, *Cell* **62**, 615 (1990); H. Nozaki, H. Kuroiwa, T. Kuroiwa, *J. Phycol.* **30**, 279 (1994).
 21. Hybridization experiments were performed as described (10), with the exception that incubation was at 55°C in Fig. 1A and at 65°C in Fig. 1B. Probes for Southern analysis were prepared as follows: in Fig. 1A, a synthetic DNA (5'-CGAAAGCCCGTTCG-GCATCAAT-3') was end-labeled with ³²P by T4 polynucleotide kinase; in Fig. 1B (left), a 616-bp DNA fragment corresponding to the internal region of the *sigA* open reading frame was amplified by PCR from the cloned *sigA* DNA with synthetic primers (5'-CAGGAACAGCTATGACCTGTCCAAACAAGTGT-GCA-3' and 5'-TGTAACACGACGGCCAGTGCAATTAACGATTCTCCC-3'), and the ³²P-labeled DNA probe was prepared by the random priming method; and in Fig. 1B (right), a 3270-bp Pst I fragment containing the *trpA* gene (11) was purified and labeled with ³²P by the random priming method.
 22. Nuclear and chloroplast DNAs were enriched by density gradient centrifugation, first on ethidium bromide-CsCl and then on Hoechst 33258-CsCl (5). Mitochondrial, chloroplast, and nuclear DNAs banded separately in this order from the top.
 23. Single-letter abbreviations for the amino acid residues are as follows: A, Ala; C, Cys; D, Asp; E, Glu; F, Phe; G, Gly; H, His; I, Ile; K, Lys; L, Leu; M, Met; N, Asn; P, Pro; Q, Gln; R, Arg; S, Ser; T, Thr; V, Val; W, Trp; and Y, Tyr.
 24. The purification of RNA polymerase core enzyme and the σ^{70} subunit has been described (16). To reconstitute the holoenzyme, we mixed the core enzyme with a threefold molar excess of either σ^{70} or SigA and then incubated the mixture for 30 min at 37°C. Single-round transcription reactions were performed under standard conditions (17). Transcripts separated by electrophoresis through a 7% polyacrylamide gel containing 8 M urea were analyzed with a Bioimage analyzer (BAS1000, Fuji Photo Film). The positions and the nucleotide length of transcripts initiated from the *tac* and RNA I promoters are indicated.
 25. Rabbit antiserum to recombinant SigA was prepared as described (18). The antiserum was passed over a protein A column and the immunoglobulin G fraction was further passed over an affinity column prepared from SigA (10 mg) conjugated with HiTrap NHS-activated (1 ml; Pharmacia) as suggested by the supplier. *C. caldarium* RK-1 cells were ground in liquid nitrogen, and an amount corresponding to 10 μ g of protein was fractionated by SDS-polyacrylamide gel electrophoresis in a 9.4% gel. Other procedures for immunoblot analysis were as described (19).
 26. Immunogold electron microscopy was performed basically as described (20). *Cyanidium* cells were fixed in 2% glutaraldehyde, embedded in LR White resin, cut with an ultramicrotome, and treated with the primary antibody. The mouse monoclonal antibodies to human double-stranded DNA were from Chemicon. After the grids were washed, immune complexes were detected through incubation for 2 hours at room temperature with antibodies to rabbit or mouse immunoglobulin G labeled with 10-nm colloidal gold particles (BioCell Research Laboratories, Cardiff, UK). The grids were then stained with 3% aqueous uranyl acetate for 20 min and examined under an electron microscope.
 27. We thank H. Hirokawa for encouragement and H. Takahashi for technical assistance. Supported in part by grants for scientific research from the Ministry of Education, Science, and Culture of Japan (05454069, 07760074, and 06101002), and by the Biodesign Research Program of RIKEN.

12 February 1996; accepted 23 April 1996

Requirement for the Adapter Protein GRB2 in EGF Receptor Endocytosis

Zhixiang Wang and Michael F. Moran*

Activated epidermal growth factor (EGF) receptors induce the formation of various complexes of intracellular signaling proteins that are mediated by SRC homology 2 (SH2) and SH3 domains. The activated receptors are also rapidly internalized into the endocytotic compartment and degraded in lysosomes. EGF stimulation of canine epithelial cells induced a rapid and transient association of the SH3-SH2-SH3 protein GRB2 with dynamin, a guanosine triphosphatase that regulates endocytosis. Disruption of GRB2 interactions by microinjection of a peptide corresponding to the GRB2 SH2 domain or its phosphopeptide ligand blocked EGF receptor endocytosis; other SH2 domains that bind EGF receptors or antibodies that neutralize RAS did not. Both activation and termination of EGF signaling appear to be regulated by the diverse interactions of GRB2.

Sites of tyrosine autophosphorylation in activated EGF receptors (EGFRs) bind and thereby activate signaling proteins that contain phosphotyrosine (pTyr)-binding domains such as SH2 and PTB domains (1). For example, the adapter proteins GRB2 and SHC bind activated EGFRs and participate in EGF-induced activation of RAS (2). Concomitant with their binding to PTB and SH2 proteins, activated EGFRs interact with adaptins (3) and are internalized by way of clathrin-coated pits into the endocytotic compartment (4). EGFR association with the adaptin AP-2 is not required for EGFR internalization (5), but receptors that lack kinase activity or pTyr sites are poorly internalized or show abnormal intracellular trafficking (6-8). Therefore, EGFR substrates or EGFR-binding signaling proteins, or both, may be required for receptor internalization and trafficking. GRB2 binds to the RAS guanine nucleotide exchange factor SOS (9) and interacts

through its SH3 domains with polyproline motifs located in the COOH-terminal regulatory region of the dynamin guanosine triphosphatase (GTPase) and with other proteins (10). Dynamin plays an essential role in coated vesicle formation (11) and localizes at the plasma membrane around the neck of emerging coated pits (12). We now show that GRB2 is required for endocytosis of the EGFR, and demonstrate a transient EGF-induced association of GRB2 with dynamin.

EGFRs are located at the surface of Maden Darby canine kidney (MDCK) cells deprived of serum. However, 30 min after stimulation with EGF, the receptors were internalized and accumulated in perinuclear vesicles characteristic of endosomes and lysosomes (Fig. 1A). When cells were microinjected (13) with a mixture of eight glutathione-S-transferase (GST) fusion peptides containing the SH2 domains of signaling proteins that bind activated EGFRs [GRB2, SHC, and two each from p120 RAS-GTPase-activating protein (RAS-GAP), the p85 α subunit of phosphatidylinositol 3-kinase (PI3K), and phospholipase C- γ 1 (PLC- γ 1)] and then

Banting and Best Department of Medical Research and Department of Molecular and Medical Genetics, University of Toronto, 112 College Street, Toronto M5G 1L6, Canada.

*To whom correspondence should be addressed.

stimulated with EGF, the receptors remained at the cell periphery (Fig. 1A). Injected cells were identified with the use of avidin-fluorescein isothiocyanate (FITC) to detect the injected biotinylated proteins, and were viewed in green fluorescence. Neighboring cells that were not microinjected with the SH2 domain peptides displayed normal EGFR endocytosis, as did cells injected with GST or a mixture of the six SH2 domains from RAS-GAP, PLC- γ 1, and PI3K (Fig. 1A); injection of these same six SH2 domains individually also did not affect EGFR internalization (14). EGFR internalization is not sensitive to the PI3K inhibitor wortmannin (7), and injection of both SH2 domains from the p85 α subunit of PI3K had no effect on EGFR internalization (Fig. 1A). However, PI3K may participate in a later stage of EGFR endocytosis, as it is

proposed to do in trafficking of the platelet-derived growth factor receptor (15).

Coinjection of the GRB2 and SHC SH2 domains or injection of the GRB2 SH2 domain alone blocked EGFR endocytosis, whereas the SHC SH2 domain by itself did not (Fig. 1, A and B). Inhibition of EGFR endocytosis by the GRB2 SH2 domain was dose-dependent, with inhibition of endocytosis apparent in ~20% of injected cells at a concentration of 0.25 mg/ml and in ~90% of injected cells at concentrations of ≥ 0.5 mg/ml (14). EGFR endocytosis was considered inhibited if the receptors remained localized at the cell periphery and were not associated with intracellular vesicles. Inhibition of EGFR endocytosis by the GRB2 SH2 domain was also apparent in Rat-2 fibroblasts (14).

Like the GRB2 SH2 domain, the SH2

domains of PLC- γ 1, SHC, RAS-GAP, and, to a lesser extent, PI3K bind pTyr sites in activated EGFRs (2, 16). Because only the GRB2 SH2 domain inhibited EGFR endocytosis, we investigated the effect of injection of a phosphopeptide ligand for this domain. Microinjection of a pTyr-containing peptide corresponding to eight residues surrounding the principal binding site (pTyr¹⁰⁶⁸) in activated EGFRs for the GRB2 SH2 domain (2) resulted in inhibition of EGFR endocytosis (Fig. 1B); the same peptide lacking the phosphate group had no effect. Thus, the inhibitory effect of the phosphopeptide was probably attributable to binding of a cellular SH2 domain protein important for EGFR endocytosis.

To investigate whether GRB2 participates in the internalization of receptors other than EGFR, we microinjected MDCK cells with

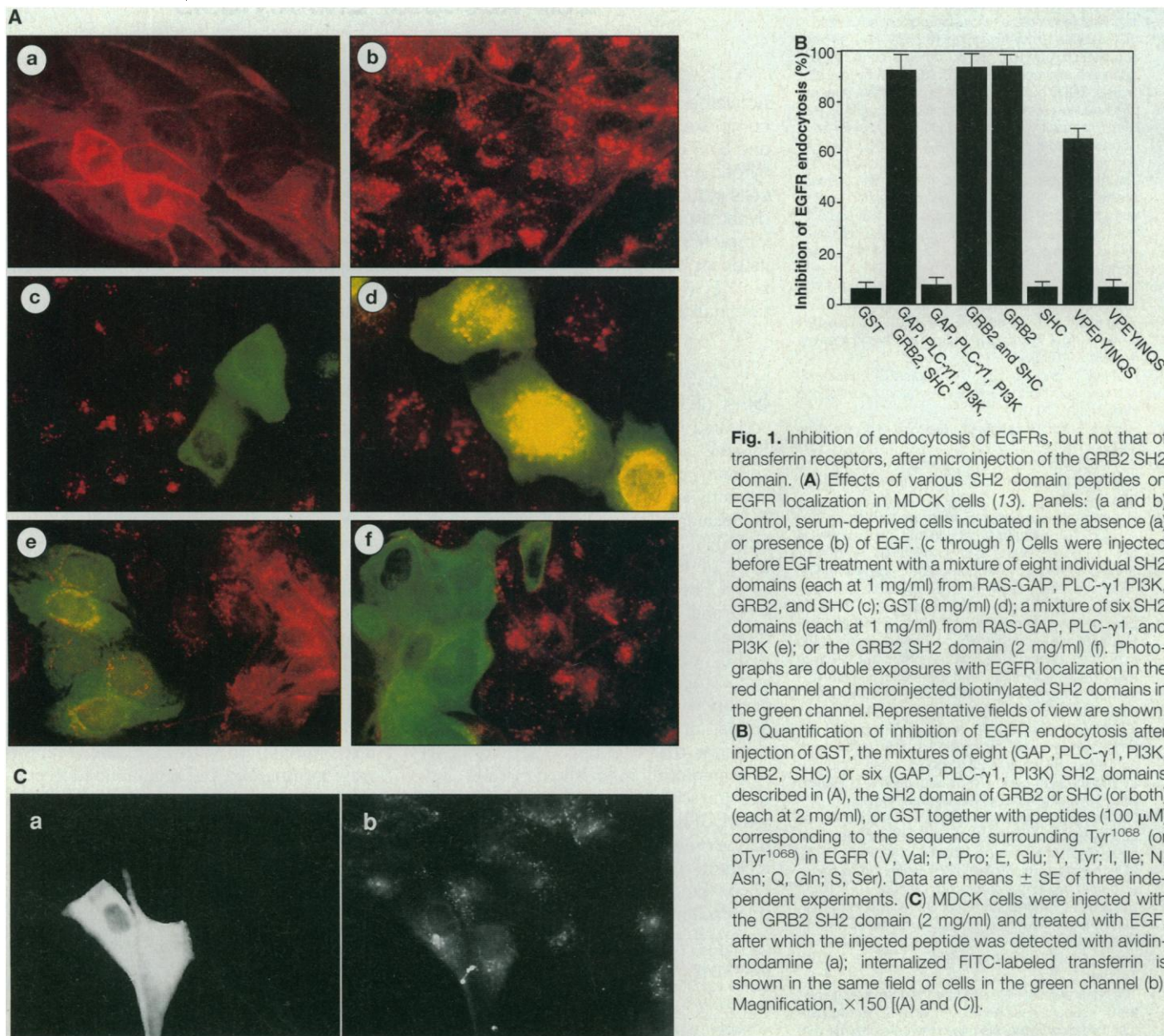


Fig. 1. Inhibition of endocytosis of EGFRs, but not that of transferrin receptors, after microinjection of the GRB2 SH2 domain. **(A)** Effects of various SH2 domain peptides on EGFR localization in MDCK cells (13). Panels: (a and b) Control, serum-deprived cells incubated in the absence (a) or presence (b) of EGF. (c through f) Cells were injected before EGF treatment with a mixture of eight individual SH2 domains (each at 1 mg/ml) from RAS-GAP, PLC- γ 1, PI3K, GRB2, and SHC (c); GST (8 mg/ml) (d); a mixture of six SH2 domains (each at 1 mg/ml) from RAS-GAP, PLC- γ 1, and PI3K (e); or the GRB2 SH2 domain (2 mg/ml) (f). Photographs are double exposures with EGFR localization in the red channel and microinjected biotinylated SH2 domains in the green channel. Representative fields of view are shown. **(B)** Quantification of inhibition of EGFR endocytosis after injection of GST, the mixtures of eight (GAP, PLC- γ 1, PI3K, GRB2, SHC) or six (GAP, PLC- γ 1, PI3K) SH2 domains described in (A), the SH2 domain of GRB2 or SHC (or both) (each at 2 mg/ml), or GST together with peptides (100 μ M) corresponding to the sequence surrounding Tyr¹⁰⁶⁸ (or pTyr¹⁰⁶⁸) in EGFR (V, Val; P, Pro; E, Glu; Y, Tyr; I, Ile; N, Asn; Q, Gln; S, Ser). Data are means \pm SE of three independent experiments. **(C)** MDCK cells were injected with the GRB2 SH2 domain (2 mg/ml) and treated with EGF, after which the injected peptide was detected with avidin-rhodamine (a); internalized FITC-labeled transferrin is shown in the same field of cells in the green channel (b). Magnification, $\times 150$ [(A) and (C)].

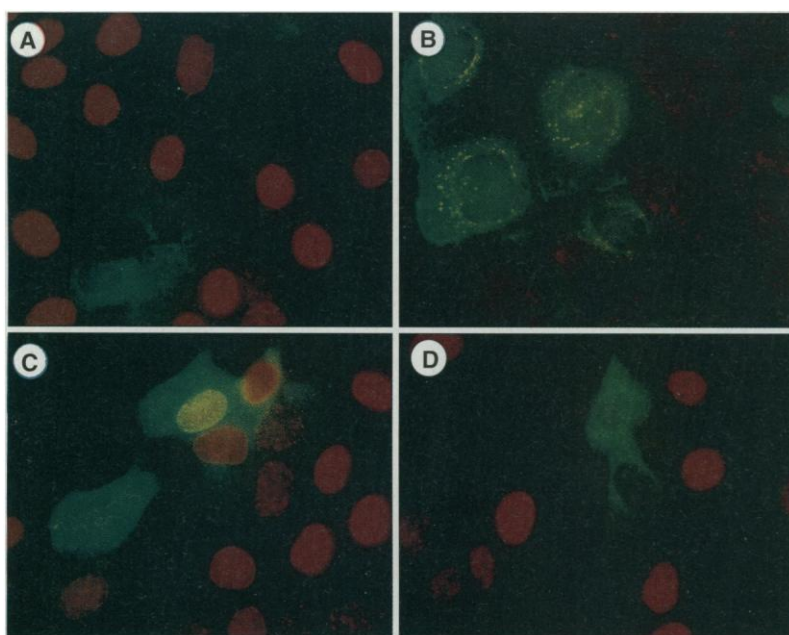
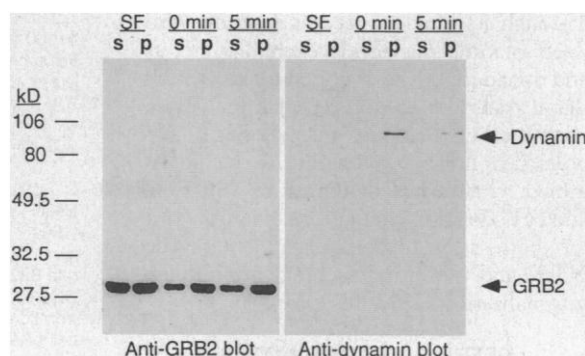


Fig. 2. Effects of microinjection with monoclonal antibodies to RAS on DNA synthesis and EGFR localization. MDCK cells were injected with monoclonal antibodies Y13-259 (**A** and **B**) or Y13-238 (**C**) or with the GRB2 SH2 domain (**D**) and stimulated with EGF. DNA synthesis was then assessed by BrdU incorporation (red channel) (**A**, **C**, and **D**) (18) and EGFR endocytosis was examined (**B**) (13). Magnification, $\times 170$.

Fig. 3. EGF-induced association of dynamin and GRB2. GRB2 was immunoprecipitated from soluble (s) and detergent-solubilized particulate (p) fractions of MDCK cells that had been incubated under serum-free conditions (SF), or incubated with EGF at 0°C for 15 min and then at 37°C for 0 or 5 min, as indicated. The immunoprecipitates were split and subjected to immunoblot analysis with antibodies to GRB2 (anti-GRB2) or to dynamin. The sizes of molecular size standards are indicated in kilodaltons.



the GRB2 SH2 domain and monitored the internalization of FITC-labeled transferrin. Although internalization of transferrin receptors, like that of EGFRs, is mediated by dynamin and clathrin-coated pits and coated vesicles, it was not disrupted by microinjection of the GRB2 SH2 domain (Fig. 1C). Thus, GRB2 is not universally required for receptor-mediated endocytosis but, rather, may participate in internalization of EGFR and perhaps other receptor tyrosine kinases. Indeed, internalization of EGFRs into coated pits requires receptor tyrosine kinase activity (7), which may reflect a dependency on specific SH2 domain-mediated interactions. FITC-conjugated EGF was internalized by receptor-mediated endocytosis and concentrated in perinuclear vesicles in MDCK cells, but not in cells microinjected with the GRB2 SH2 domain (14). These data and analysis of EGFR localization at several time points ranging from 5 to 60 min after EGF treatment (14) indicated that receptor-mediated endocytosis of EGF is blocked, and not simply delayed or replaced by receptor recycling, in cells injected with the GRB2 SH2 domain.

Given the role of RAS-related GTPases in vesicle trafficking, and the fact that GRB2 participates in EGF-induced activation of RAS, we investigated whether RAS was required for EGFR endocytosis. Microinjection of the Y13-259 neutralizing monoclonal antibody to Ras, but not the Y13-238 monoclonal antibody to Ras, blocks growth factor-induced cell proliferation (17). Injection of Y13-259, but not Y13-238, inhibited EGF-induced DNA synthesis in MDCK cells (18) (Fig. 2). However, neither Y13-259 (Fig. 2) nor Y13-238 (14) interrupted EGFR endocytosis in these cells. Thus, EGFR internalization and localization to perinuclear endosomes is not dependent on RAS signaling, and therefore GRB2 function in endocytosis

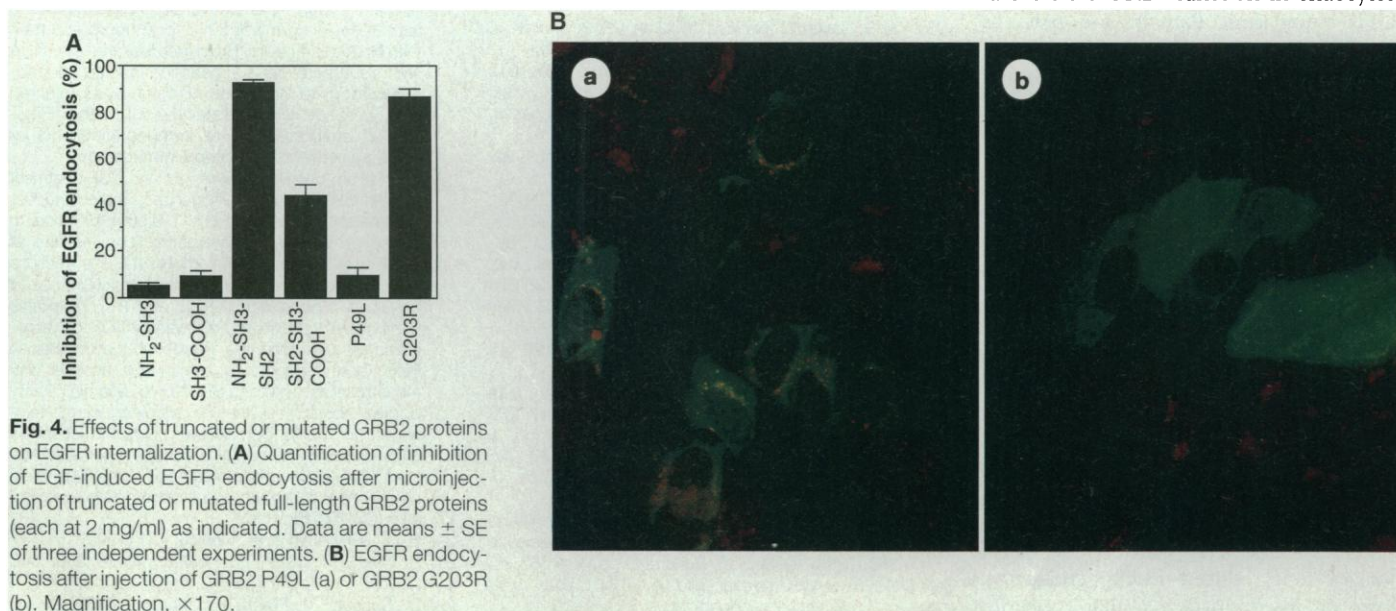


Fig. 4. Effects of truncated or mutated GRB2 proteins on EGFR internalization. (**A**) Quantification of inhibition of EGF-induced EGFR endocytosis after microinjection of truncated or mutated full-length GRB2 proteins (each at 2 mg/ml) as indicated. Data are means \pm SE of three independent experiments. (**B**) EGFR endocytosis after injection of GRB2 P49L (**a**) or GRB2 G203R (**b**). Magnification, $\times 170$.

is likely independent of interaction of GRB2 with SOS. The ability of the injected GRB2 SH2 domain to inhibit EGF-induced DNA synthesis (Fig. 2) may reflect disruption of the GRB2-mediated activation of RAS.

To determine whether GRB2 participates in EGFR endocytosis through interaction with dynamin, we examined the effect of EGF on the association of these two proteins. Equal amounts of GRB2 were recovered by immunoprecipitation from soluble and particulate fractions of MDCK cells deprived of serum. However, treatment of cells with EGF induced a redistribution of GRB2, such that ~70% of the protein partitioned with the particulate fraction (Fig. 3) (19). Dynamin was not detected in GRB2 immune complexes from unstimulated cells. However, treatment of cells with EGF resulted in association of dynamin with GRB2 in the particulate, but not in the soluble, fraction (Fig. 3). Under the experimental conditions used (treatment with EGF at 0°C), the EGFR undergoes autophosphorylation, but receptor internalization is blocked. Subsequent incubation of the EGF-treated cells at 37°C for 5 min was accompanied by a decrease in the amount of dynamin recovered in the GRB2 immune complex from the particulate fraction. These results demonstrate a transient EGF-induced association of GRB2 and dynamin, which is likely mediated by one or both SH3 domains of GRB2. The observation that the GRB2-dynamin complex was restricted to the particulate fraction is consistent with a functional role for this complex in EGFR internalization.

GRB2 consists of a single SH2 domain and two SH3 domains in the order NH₂-SH3-SH2-SH3-COOH (20, 21). The GRB2 SH2 domain binds preferentially to pTyr groups that are two residues upstream of an Asn; such sequences are present in the EGFR cytoplasmic domain and SHC (2). The NH₂-terminal SH3 domain of GRB2 interacts with SOS and CBL and is important in RAS-dependent vulval development in *Caenorhabditis elegans* (21, 22). To confirm that GRB2 itself and not simply a GRB2 SH2 binding site participates in EGFR endocytosis, and to test the hypothesis that one or both GRB2 SH3 domains interact with an endocytosis factor, we microinjected truncated versions of GRB2 into MDCK cells. Injection of either SH3 domain from GRB2 had no inhibitory effect on EGFR endocytosis (Fig. 4A), possibly because they lack the localization signal provided by the SH2 domain (23). We anticipated that injection of a GRB2 SH3 domain joined to the SH2 domain might be functional rather than inhibitory. Injection of the NH₂-SH3-SH2 portion of GRB2 blocked EGF-induced EGFR endocytosis. However, injection of a similar concentra-

tion (verified by in vitro binding experiments) of SH2-SH3-COOH resulted in only partial inhibition; about half of the injected cells showed EGFR endocytosis (Fig. 4A). We interpreted this latter result to mean that SH2-SH3-COOH participated in EGFR endocytosis and did not function in a dominant negative manner. Results consistent with this interpretation were obtained by injection of full-length GRB2 containing SH3 domains expected to be defective on the basis of mutated forms of the *C. elegans* GRB2 homolog SEM-5 (21). Full-length GRB2 G203R (Gly²⁰³ → Arg), which contains wild-type NH₂-SH3 and SH2 domains and a defective SH3-COOH domain, inhibited EGFR endocytosis to the same extent as the SH2 and NH₂-SH3-SH2 constructs, presumably by displacing endogenous GRB2 (Fig. 4). However, full-length GRB2 P49L (Pro⁴⁹ → Leu), which contains a defective NH₂-SH3 domain joined to wild-type SH2 and SH3-COOH domains, had no effect on EGFR endocytosis (Fig. 4). These results implicate the SH3-COOH domain of GRB2 in EGFR endocytosis.

Dynamin may be subject to multiple forms of regulation, and GRB2 may exert effects in growth factor-stimulated cells. Through its EGF-induced association with RAS guanine nucleotide exchange factors and dynamin, GRB2 is poised to affect both signal transduction and receptor endocytosis. Whether these are independent or coordinated functions remains to be determined. Our results demonstrate that SH2 and SH3 domain interactions are important for both transmitting signals from the EGFR and inhibiting such signals through internalization of the receptor.

REFERENCES AND NOTES

1. T. Pawson, *Nature* **373**, 573 (1995).
2. A. G. Batzer, D. Rotin, J. M. Urena, E. Y. Skolnik, J. Schlessinger, *Mol. Cell. Biol.* **14**, 5192 (1994).
3. A. Sorkin and G. Carpenter, *Science* **261**, 612 (1993).
4. G. Di Guglielmo, P. Baass, W. Ou, B. Posner, J. Bergeron, *EMBO J.* **13**, 4269 (1994).
5. A. Nesterov *et al.*, *Proc. Natl. Acad. Sci. U.S.A.* **92**, 8719 (1995).
6. S. J. Decker *et al.*, *J. Biol. Chem.* **267**, 1104 (1992); K. Helin and L. Beguinot, *ibid.* **266**, 8363 (1991); A. Sorkin, K. Helin, C. M. Waters, G. Carpenter, L. Beguinot, *ibid.* **267**, 8672 (1992); C. Chang *et al.*, *ibid.* **268**, 19312 (1993); J. R. Glenney *et al.*, *Cell* **52**, 675 (1988); W. Chen *et al.*, *ibid.* **59**, 33 (1989); H. S. Wiley *et al.*, *J. Biol. Chem.* **266**, 11083 (1991).
7. C. Lamaze and S. Schmid, *J. Cell Biol.* **129**, 47 (1995).
8. S. Felder *et al.*, *Cell* **61**, 623 (1990); S. Felder, J. La Vin, A. Ullrich, J. Schlessinger, *J. Cell Biol.* **117**, 203 (1992); A. M. Honegger, R. M. Kris, A. Ullrich, J. Schlessinger, *Proc. Natl. Acad. Sci. U.S.A.* **86**, 925 (1989); A. Honegger, A. Schmidt, A. Ullrich, J. Schlessinger, *J. Cell Biol.* **110**, 1541 (1990).
9. J. P. Olivier *et al.*, *Cell* **73**, 179 (1993); L. Buday and J. Downward, *ibid.*, p. 611; P. Chardin *et al.*, *Science* **260**, 1338 (1993); S. E. Egan *et al.*, *Nature* **363**, 45 (1993); N. W. Gale *et al.*, *ibid.*, p. 88; N. Li *et al.*, *ibid.*, p. 85; M. Rozakis-Adcock *et al.*, *ibid.*, p. 83.

10. I. Gout *et al.*, *Cell* **75**, 25 (1993); J. Herskovits, H. Shpetner, C. Burgess, R. Vallee, *Proc. Natl. Acad. Sci. U.S.A.* **90**, 11468 (1993); C. David, P. McPherson, O. Mundigl, P. De Camilli, *ibid.* **93**, 331 (1996); K. Seedorf *et al.*, *J. Biol. Chem.* **269**, 16009 (1994); R. Scaife, I. Gout, M. Waterfield, R. Margolis, *EMBO J.* **13**, 2574 (1994); P. McPherson, K. Takei, S. Schmid, P. De Camilli, *J. Biol. Chem.* **269**, 30132 (1994); H. Miki *et al.*, *ibid.*, p. 5489; A. Ando *et al.*, *EMBO J.* **13**, 3033 (1995).
11. A. van der Bliek *et al.*, *J. Cell Biol.* **122**, 553 (1993); J. S. Herskovits *et al.*, *ibid.*, p. 565; H. Damke *et al.*, *ibid.* **127**, 925 (1994).
12. J. Hinshaw and S. Schmid, *Nature* **374**, 190 (1995); K. Takei, P. McPherson, S. Schmid, P. De Camilli, *ibid.*, p. 86.
13. MDCK cells plated on cover slips were deprived of serum overnight and then microinjected with biotinylated GST fusion peptides containing various SH2 domains. Cells were injected with ~1 fl of 0.5× phosphate-buffered saline containing the indicated peptides or biotinylated GST. After microinjection, cells were incubated at 37°C for 1 hour, and then treated with EGF (100 ng/ml) at 0°C for 15 min (24). The EGF-containing medium was then replaced with warm Dulbecco's modified Eagle's medium, and cells were incubated at 37°C for 30 min. After fixation and permeabilization (24), the cells were incubated first with sheep polyclonal antibodies to EGFRs (Upstate Biotechnology) that had been preabsorbed with GST beads, and then with a mixture of FITC-labeled avidin (to stain microinjected cells) and rhodamine-labeled donkey antibodies to sheep immunoglobulin G (to stain EGFRs) (Jackson Immunology). Color photographs were taken by double exposure with two channels (FITC and rhodamine). For quantification of inhibition of EGFR endocytosis, the percentage of injected cells in which EGFR endocytosis was disrupted was determined by multiplying the number of microinjected cells in which EGFR internalization was blocked by 100 and dividing by the total number of injected cells. For each experiment, 200 to 300 cells were microinjected with a given solution.
14. Z. Wang and M. F. Moran, unpublished data.
15. M. Joly, A. Kazlauskas, F. Fay, S. Corvera, *Science* **263**, 684 (1994); M. Joly, A. Kazlauskas, S. Corvera, *J. Biol. Chem.* **270**, 13225 (1995).
16. D. Rotin *et al.*, *EMBO J.* **11**, 559 (1992); C. Soler, L. Beguinot, G. Carpenter, *J. Biol. Chem.* **269**, 12320 (1994).
17. M. R. Smith, S. J. DeGudicibus, D. W. Stacey, *Nature* **320**, 540 (1986).
18. DNA synthesis was assayed after metabolic incorporation of bromodeoxyuridine (BrdU) (Amersham cell proliferation kit). MDCK cells were deprived of serum overnight and then microinjected with antibodies to RAS (2 mg/ml) or biotinylated GRB2 SH2 domain (2 mg/ml). The cover slips were incubated with EGF (50 ng/ml) at 37°C for 6 hours and then with BrdU for 4 hours. BrdU incorporated into DNA was visualized with a rhodamine-labeled secondary antibody to mouse immunoglobulin G. Injected cells were identified by staining with either FITC-labeled antibodies to rat immunoglobulin G or FITC-labeled avidin (Jackson Immunology).
19. After serum deprivation overnight and EGF treatment (73), MDCK cells were homogenized. The postnuclear supernatant was centrifuged at 100,000g for 1 hour to yield the soluble and particulate fractions, the latter of which was solubilized with 1% NP-40. The fractions were then subjected to immunoprecipitation with rabbit polyclonal antibodies to GRB2, and the precipitates were washed extensively, resolved by SDS-polyacrylamide gel electrophoresis, transferred to nitrocellulose filters, and subjected to immunoblot analysis with monoclonal antibodies to GRB2 or to dynamin (Transduction Laboratories). Immune complexes were detected with horseradish peroxidase-conjugated secondary antibodies and chemiluminescence reagents (Amersham). Images were captured on RP film (Kodak) and chemiluminescence was quantified with a Molecular Imager (GS-250; Bio-Rad).
20. E. J. Lowenstein *et al.*, *Cell* **70**, 431 (1992).
21. S. Clark, M. Stern, H. Horvitz, *Nature* **356**, 340 (1992).
22. D. Cussac, M. Frech, P. Chardin, *EMBO J.* **13**,

- 4011 (1994); T. Raabe *et al.*, *ibid.* **14**, 2509 (1995); H. Yu *et al.*, *Science* **258**, 1665 (1992); J. Donovan, R. Wange, W. Langdon, L. Samelson, *J. Biol. Chem.* **269**, 22925 (1994); H. Meisner and M. Czeck, *ibid.* **270**, 25332 (1995).
23. D. Bar-Sagi, D. Rotin, A. Batzer, V. Mandiyan, J. Schlessinger, *Cell* **74**, 83 (1993).
24. Z. Wang, P. S. Tung, M. F. Moran, *Cell Growth Different.* **7**, 123 (1996).
25. We thank J. Schlessinger and A. Batzer for GRB2

reagents, D. Bar-Sagi for advice on cell microinjection, and T. Pawson, J. McClade, M. Tyers, and C. J. Ingles for comments on the manuscript. Supported in part by Ciba-Geigy Canada and grants from the Canadian Cancer Society and Medical Research Council. M.F.M. is a National Cancer Institute of Canada Scientist, and Z.W. is a Charles H. Best Foundation Fellow.

11 January 1996; accepted 2 May 1996

Antiviral Effect and Ex Vivo CD4⁺ T Cell Proliferation in HIV-Positive Patients as a Result of CD28 Costimulation

Bruce L. Levine, Joseph D. Mosca, James L. Riley, Richard G. Carroll, Maryanne T. Vahey, Linda L. Jagodzinski, Kenneth F. Wagner, Douglas L. Mayers, Donald S. Burke, Owen S. Weislow, Daniel C. St. Louis, Carl H. June*

Because stimulation of CD4⁺ lymphocytes leads to activation of human immunodeficiency virus-type 1 (HIV-1) replication, viral spread, and cell death, adoptive CD4⁺ T cell therapy has not been possible. When antigen and CD28 receptors on cultured T cells were stimulated by monoclonal antibodies (mAbs) to CD3 and CD28 that had been immobilized, there was an increase in the number of polyclonal CD4⁺ T cells from HIV-infected donors. Activated cells predominantly secreted cytokines associated with T helper cell type 1 function. The HIV-1 viral load declined in the absence of antiretroviral agents. Moreover, CD28 stimulation of CD4⁺ T cells from uninfected donors rendered these cells highly resistant to HIV-1 infection. Immobilization of CD28 mAb was crucial to the development of HIV resistance, as cells stimulated with soluble CD28 mAb were highly susceptible to HIV infection. The CD28-mediated antiviral effect occurred early in the viral life cycle, before HIV-1 DNA integration. These data may facilitate immune reconstitution and gene therapy approaches in persons with HIV infection.

CD4⁺ T cells contain the major reservoir of HIV-1 in vivo (1, 2). The difficulties involved in inducing proliferation in vitro of autologous CD4⁺ T cells from patients with HIV-1 infection limit the therapeutic potential for many approaches that involve gene therapy or immune reconstitution of infected persons (3). Two obstacles attributed to impaired CD4⁺ T cell proliferation are a limited clonogenic potential of the uninfected CD4 and CD8 cells and the activation of HIV-1 expression and viral production (4). In addition to T cell receptor (TCR) engagement of an antigenic peptide

bound to major histocompatibility complex (MHC) receptors, other costimulatory signals are necessary for T cell activation. The most important of the costimulatory signals identified to date is provided by the interaction of CD28 on T cells with its ligands CD80 and CD86 on antigen-presenting cells (5). Because CD28 signal transduction can prevent apoptosis in cultures of HIV-infected cells and can induce expression of the *Bcl-X_L* cell survival gene (6), we tested the hypothesis that costimulation might be limiting in cultures from HIV-infected patients.

We cultured lymphocytes from 10 patients with HIV-1 infection (CD4 counts of 350 to 600 cells/mm³) in the presence of beads coated with CD3 mAb OKT3 and CD28 mAb 9.3 (Table 1). Cell culture was performed in the absence of exogenous cytokines or feeder cells, as CD28 stimulation provides the necessary costimulus to replace feeder cells (7). Figure 1 shows the growth curve of CD4⁺ T cells from an HIV-infected patient after stimulation by a conventional method [with phytohemagglutinin (PHA) and interleukin-2 (IL-2)] or with CD3 and CD28 mAbs in medium that did not contain antiretroviral agents. In the PHA-stimulated

culture, the growth curve revealed an initial exponential expansion and a subsequent plateau phase, resulting in termination on day 18 of the culture (Fig. 1A). This pattern was coincident with increased p24 antigen production and with increased viral burden as measured by a quantitative polymerase chain reaction (PCR) for cellular HIV-1 *gag* (Fig. 1, B to D). In contrast, when cells were cultured with CD3 and CD28 mAbs, exponential cell proliferation was maintained for 50 days (Fig. 1A). Although there was evidence of modest viral expression early in the culture, as indicated by the concentration of p24 on day 8 (Fig. 1B), viral production and proviral DNA decreased to undetectable amounts in the culture (Fig. 1, C and D). Similar results were obtained whether the starting cell population was peripheral blood mononuclear cells (PBMCs) or purified CD4⁺ T cells; this finding suggested that the enhanced cell proliferation and antiviral effects in the culture stimulated with CD3 and CD28 mAbs were not dependent on CD8⁺ T cells or accessory cells (Table 2) (8).

A quantitative PCR was used to determine amounts of HIV-1 *gag* DNA and RNA in the cultures of lymphocytes from the 10 HIV-positive patients (Table 1). Culture with CD28 mAb resulted in decreased viral burden in all patient-derived cells, including the cells cultured in the absence of antiretroviral agents. HIV-1 *gag* proviral DNA became undetectable in six of seven cultures from patients that were cultured in the absence of antiretroviral agents, and HIV-1 *gag* RNA became undetectable in five of the seven cultures. Culture supernatants were also sampled for p24 antigen at 7- to 14-day intervals. Antigen was not detected in 9 of the 10 patients; in one patient (patient 9; Table 1 and Fig. 1), decreasing concentrations of p24 antigen with time were detected. Virus-free CD4⁺ T cell proliferation also occurred even when CD8 cells constituted <1% of the cells (Table 2) (9).

The increase in the number of CD4 cells was not significantly different in the presence or absence of a combination of antiretroviral agents in three patients (8). In uninfected adult blood donors, the average absolute magnitude of the CD28-mediated proliferation of ex vivo polyclonal CD4⁺ T cells is ~10¹⁰ or 33 population doublings (7). The limits of CD4⁺ T cell proliferation in HIV-infected patients have not yet been determined, because 7 of 10 cultures were terminated after 4 to 8 weeks of culture and cell proliferation remained in the exponential phase. However, the observed increase appeared to be substantial, with a geometric mean expansion of 6.7 log units in the two CD4⁺ cell cultures that were continued to plateau phase (Table 1). The mean percent-

B. L. Levine and C. H. June, Naval Medical Research Institute, Bethesda, MD 20889, USA.

J. D. Mosca, R. G. Carroll, L. L. Jagodzinski, K. F. Wagner, D. C. St. Louis, Henry M. Jackson Foundation for the Advancement of Military Medicine, Rockville, MD 20850, USA.

J. L. Riley, M. T. Vahey, D. S. Burke, Division of Retrovirology, Walter Reed Army Institute for Research, Rockville, MD 20850, USA.

D. L. Mayers, Naval Medical Research Institute, Bethesda, MD 20889, USA, and Division of Retrovirology, Walter Reed Army Institute for Research, Rockville, MD 20850, USA.

O. S. Weislow, Life Sciences Division, SRA Technologies, Rockville, MD 20850, USA.

*To whom correspondence should be addressed.